

Robust low-rank covariance matrix estimation with a general pattern of missing values

A. Hippert-Ferrer^{a,b}, M. N. El Korso^b, A. Breloy^b, G. Ginolhac^c

^a*L2S, Paris Saclay University, 3 rue Joliot Curie, 91190 Gif-sur-Yvette, France*

^b*LEME, Paris-Nanterre University, 50 rue de Sèvres, 92410 Ville d'Avray, France*

^c*LISTIC, Savoie Mont Blanc University, 5 chemin de Bellevue, Annecy, France*

Abstract

This paper tackles the problem of robust covariance matrix estimation when the data is incomplete. Classical statistical estimation methodologies are usually built upon the Gaussian assumption, whereas existing robust estimation ones assume unstructured signal models. The former can be inaccurate in real-world data sets in which heterogeneity causes heavy-tail distributions, while the latter does not profit from the usual low-rank structure of the signal. Taking advantage of both worlds, a covariance matrix estimation procedure is designed on a robust (compound Gaussian) low-rank model by leveraging the observed-data likelihood function within an expectation-maximization algorithm. It is also designed to handle general pattern of missing values. The proposed procedure is first validated on simulated data sets. Then, its interest for classification and clustering applications is assessed on two real data sets with missing values, which include multispectral and hyperspectral time series.

Keywords: Missing data, covariance matrix, compound Gaussian, low-rank, expectation-maximization algorithm, classification.

1. Introduction

Missing data appear when no value of the data is available for a given variable and a given observation. This classical problem [1, 2] is a pitfall in statistical signal processing and its related fields, as statistical inference [3, 4] and data analysis [5, 6]. To

^{*}This work was supported by ANR ASTRID project MARGARITA (ANR-17-ASTR-0015).

name a few applications where missing data has drawn significant attention, we can cite biomedical studies, chemometrics [7] or remote sensing where missing values created by poor atmospheric conditions or sensor failure can dramatically hinder the understanding of the physical phenomenon under observation [8]. Covariance matrix (CM) estimation theory, which is a fundamental issue in signal processing and machine learning problems, has witnessed particular efforts focusing in the case of incomplete data.

In this scope, it is known that any efficient estimation algorithm should be able to exploit the source of information offered by missing values, which is formerly called *informative missingness* [9]. One approach to estimate the CM with missing values is to rely on maximum likelihood (ML) estimation with a prior assumption on the probability distribution of the data. Within this framework, the Expectation-Maximization (EM) algorithm [10] is a handy iterative procedure to obtain ML estimates as it is based on the expectation of the conditional probability $p(\mathbf{z}|\mathbf{x}, \boldsymbol{\theta})$ of the latent (missing) variables \mathbf{z} given the observed variables \mathbf{x} and the parameters $\boldsymbol{\theta}$ under estimation. Extensive work has been put into CM estimation with missing values using the EM algorithm by assuming independent and identically distributed (iid) samples drawn from the Gaussian distribution with regular sample size (i.e. $n > p$) [11, 12] or in high-dimensional regime [13, 14, 15] ($p > n$). Other models have been considered in which the covariance is assumed to have a low-rank plus identity structure [14], which will be referred in the following to as LR structure¹. This structure is closely related to signal subspace inference or principal component analysis (PCA) with missing values [16, 17].

To overcome robustness issues associated with the classical Gaussian assumption, more general distributions have been considered, such as the multivariate t -distribution [18, 19] and its regularized version for small sample size using an improved EM algorithm [20]. These distributions are encompassed by elliptical symmetric (ES) distributions, which are directly linked via ML estimation to the so-called M-estimators in the complete data case [21, 22, 23]. The robustness of these tools to non-Gaussianity [24] has been illustrated in a wide range of applications including radar processing, hyperspectral imagery and classification [25, 26, 27, 28]. One important class of ES distribution are compound Gaussian (CG) distributions [29] which are known to provide a better fit to

¹It is sometimes named spiked or factor model.



Figure 1: Illustration of three rectangular data sets with different missing data patterns (black=observed, white=missing): monotone, general and random. Note that the random pattern is a special case of the general pattern, where missing values appear on individual observations rather than blocks. See [34] (p. 5) for a precise description of missing data patterns.

empirical measurements in heterogeneous environments [30].

This paper proposes to take advantage of both robust estimation and LR structure models by proposing a EM-based procedure to estimate the CM in the case of incomplete data drawn from a CG distribution. As cited above, existing robust covariance estimation algorithms based on CG distributions are not designed to deal with missing values, and, to the best of our knowledge, existing works which use the LR structure are only based on Gaussian assumptions. In the full rank case, the work of [31] has extended generalized elliptical distributions (GES), from which CG distributions are a sub-class, to incomplete data by proposing an adapted form of the Tyler’s M-estimator.

Furthermore, existing estimation algorithms that deal with missing data assume that the missingness pattern, i.e. the pattern describing which values are missing with respect to the observed data, is a monotone pattern [18, 12, 20, 31] (see the illustration of missing data patterns in Fig. 1). This pattern can be of interest, e.g. in longitudinal studies [32] or sensor failure [33]. However, in other applications such as remote sensing, missing values can take very diverse patterns because of unpredictable events (clouds, snowfall, etc.) [8], which leads to the so-called general pattern [3].

With the previous points in mind concerning *i)* robustness to non-Gaussianity, *ii)* low-rank structured models and *iii)* missingness patterns, the contributions of this paper are summarized hereafter:

- 1) A generic algorithm for CM estimation is developed for structured signals with a non-Gaussian distribution. A procedure for non-structured / Gaussian is also obtained as a special case. In the structured configuration, the covariance matrix is supposed to have a LR structure as in [35], which will be detailed in the next section;

- 2) The analysis of missingness patterns is extended to the general pattern, which fills a gap in robust estimation;
- 3) The proposed estimators are tested on both simulated and real data sets with two applications in machine learning, namely supervised classification and unsupervised clustering with missing values, which has rarely been applied outside of simulated data in the literature of CM estimation with missing values.

The rest of the paper is organized as follows: Section 2 formulates the problem by detailing the CG distribution, the LR CM structure and the missing data model. Section 3 describes the proposed robust CM estimation procedures for unstructured and structured models. Section 4 illustrates the performance of the proposed method on simulated data sets in terms of CM estimation and data imputation. Finally, Section 5 shows the interest of the proposed procedure in real data applications using covariance-based machine learning methods.

Notations. a indicates a scalar quantity, \mathbf{a} represents a vector quantity and \mathbf{A} a matrix. $\{a_i\}_{i=1}^n$ denotes the set of elements a_i with $i \in [1, n]$. The transpose operator is \top , whereas $\text{tr}\{\cdot\}$ and $|\cdot|$ are respectively the trace and the determinant operators. The eigenvalue decomposition is denoted by $\stackrel{\text{EVD}}{=}.$ \succeq indicates positive definitiveness, \mathcal{S}_{++}^p is the set of $p \times p$ symmetric positive definite (SPD) matrices² and $\text{St}_{p,r}$ is the real Stiefel manifold of $p \times r$ orthogonal matrices³. \propto stands for ‘‘proportional to’’. $Q(\cdot)$ is the score function. Finally, $\mathbb{E}[\cdot]$ denotes the expectation operator.

2. Problem formulation

2.1. Compound Gaussian distributions

Most of covariance matrix estimation procedures with incomplete data use the Gaussian assumption. However, this assumption can be inaccurate in remote sensing applications, where images often include heterogeneous areas. The compound Gaussian (CG) distributions can tackle this issue by managing heavier tails, which offers a better fit

² $\mathcal{S}_{++}^p = \{\mathbf{\Sigma} \in \mathcal{S}_p : \forall \mathbf{x} \in \mathbb{R}^p \setminus \{0\}, \mathbf{x}^\top \mathbf{\Sigma} \mathbf{x} > 0\}.$

³ $\text{St}_{p,r} = \{\mathbf{U} \in \mathbb{R}^{p \times r} : \mathbf{U}^\top \mathbf{U} = \mathbf{I}_r\}.$

to empirical data [29]. A real p -vector $\mathbf{y} \in \mathbb{R}^p$ follows a zero-mean multivariate CG distribution, denoted $\mathbf{y} \sim \mathcal{CG}(\mathbf{0}, \mathbf{\Sigma}, f_\tau)$ if it admits the stochastic representation

$$\mathbf{y} = \sqrt{\tau} \mathbf{n} \quad (1)$$

with $\mathbf{n} \sim \mathcal{N}(\mathbf{0}, \mathbf{\Sigma})$ and for some positive real random scalar τ , called the *texture*, independent from \mathbf{n} and with PDF $f_\tau(\cdot)$. Note that the type of distribution within the class of CG distributions is mainly guided by the assumption on the PDF function [29].

Let us now define a rectangular data set $\mathbf{Y} \in \mathbb{R}^{p \times n}$ represented by $\mathbf{Y} = \{\mathbf{y}_i = (y_{1,i}, y_{2,i}, \dots, y_{p,i})^\top\}$ where $\{\mathbf{y}_i\}_{i=1}^n$ are modeled as n iid vectors of dimension p drawn from a CG distribution. To avoid any prior on the distribution of the texture parameter, the CG model can be generalized by assuming that $\{\tau_i\}$ are strictly positive, deterministic and unknown variables⁴. This leads to the following model:

$$\mathbf{y}_i | \tau_i \sim \mathcal{N}(\mathbf{0}, \tau_i \mathbf{\Sigma}), \quad \mathbf{\Sigma} \subseteq \mathcal{S}_{++}^p, \quad \tau_i > 0 \quad (2)$$

The likelihood function of model (2) is given by

$$\mathcal{L}(\mathbf{y}_i | \mathbf{\Sigma}, \tau_i) \propto \prod_{i=1}^n |\tau_i \mathbf{\Sigma}|^{-1} \exp(-\mathbf{y}_i^\top (\tau_i \mathbf{\Sigma})^{-1} \mathbf{y}_i) \quad (3)$$

Such model is sometimes referred to as scaled-Gaussian (SG) because the texture can be seen as a *scale* setting of the Gaussian model [38]. The latter will be referred to as CG for convenience. As already mentioned, this distribution is more robust than the purely Gaussian one because the scales allow flexibility in the presence of heterogeneous data, e.g. noisy data, possible outliers or inconsistencies in the data.

Remark 1. As it is clear that $\tau_i = 1, \forall i$ in the deterministic CG distribution (2) gives the Gaussian distribution, results regarding CM estimation will be given by considering the Gaussian distribution as a special case of the CG distribution.

⁴This model, which has proven its convenience in [21], follows a parametrisation of the covariance matrix of the real elliptical model $\mathcal{E}(\mathbf{0}, \tau \boldsymbol{\xi})$, where $\boldsymbol{\xi}$ is the shape matrix and where τ has only one value. In our case, the scale parameter varies at each observation $i = 1, \dots, n$. More details can be found in [36, 24, 37].

Here we assume that Σ is characterized by a LR structure which can be modeled by the well-known factor model [39] (also known as spiked model [40]):

$$\begin{cases} \Sigma = \sigma^2 \mathbf{I}_p + \mathbf{H} \\ \mathbf{H} \succeq \mathbf{0} \\ \text{rank}(\mathbf{H}) = r \\ \sigma > 0 \end{cases} \quad (4)$$

where \mathbf{I}_p denotes the p -dimensional identity matrix and \mathbf{H} is a $p \times p$ low-rank signal covariance matrix of rank r . As in many works, the latter is considered to be known from prior physical assumptions [35] or pre-estimated as in model order selection techniques [41]. Model (4) is directly related to principal component analysis (PCA) and subspace recovery [42].

2.2. Data model

As each vector \mathbf{y}_i might have missing elements, it is necessary to design a model that takes into account incompleteness. Thereby, each of its observed and missing elements can be grouped in vectors denoted by \mathbf{y}_i^o and \mathbf{y}_i^m respectively, which are stacked in vectors $\tilde{\mathbf{y}}_i$ such that

$$\tilde{\mathbf{y}}_i = \mathbf{P}_i \mathbf{y}_i = \begin{pmatrix} \mathbf{y}_i^o \\ \mathbf{y}_i^m \end{pmatrix}, \quad i = 1, \dots, n \quad (5)$$

where $\mathbf{P}_i \in \mathbb{R}^{p \times p}$ denotes a permutation matrix⁵. As illustrated by Fig. 2, this set of operations consists in permuting the missing elements at the bottom of each vector \mathbf{y}_i . Then, the covariance matrix of $\tilde{\mathbf{y}}_i$ becomes

$$\tilde{\Sigma}_i = \begin{pmatrix} \tilde{\Sigma}_{i,oo} & \tilde{\Sigma}_{i,mo} \\ \tilde{\Sigma}_{i,om} & \tilde{\Sigma}_{i,mm} \end{pmatrix} = \mathbf{P}_i \Sigma \mathbf{P}_i^\top \quad (6)$$

where $\tilde{\Sigma}_{i,mm}$, $\tilde{\Sigma}_{i,mo}$, $\tilde{\Sigma}_{i,oo}$ are the block CM of \mathbf{y}_i^m , of \mathbf{y}_i^m and \mathbf{y}_i^o , and of \mathbf{y}_i^o .

In a similar manner, the recent work of [43] uses a $n_i \times p$ selection matrix \mathbf{A}_i constructed from \mathbf{I}_p , which gives an alternative view of the problem. However, these results

⁵Note that \mathbf{P}_i is invertible and $\mathbf{P}_i^{-1} = \mathbf{P}_i^\top$.

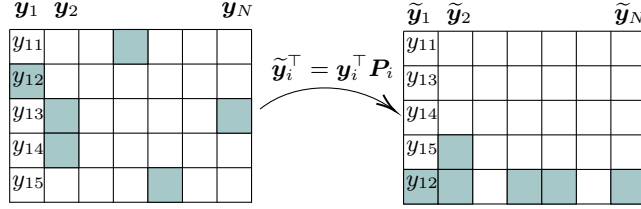


Figure 2: Missing elements (colored) of each \mathbf{y}_i are permuted to fall at the bottom of each $\tilde{\mathbf{y}}_i$. Indeed, a completely observed \mathbf{y}_i implies that $\mathbf{P}_i = \mathbf{I}_p$.

hold for the Gaussian distribution. It should also be mentioned that since each \mathbf{y}_i follows a CG distribution, their permuted version $\tilde{\mathbf{y}}_i$ also follow a CG distribution because only elements within each p -vector are permuted.

2.3. The EM algorithm: a brief reminder

The EM algorithm is a widely employed iterative scheme for ML estimation in incomplete-data problems [10]. This algorithm offers a rigorous and formal approach to the intuitive *ad hoc* idea of filling in missing values⁶: at the E-step, the following conditional expectation of the complete-data loglikelihood is found given the observed data and the current estimated parameters $\boldsymbol{\theta}$:

$$\mathcal{L}_c(\boldsymbol{\theta}|\mathbf{Y}) = \log \mathcal{L}(\mathbf{y}_i|\boldsymbol{\Sigma}, \tau_i) \quad (7)$$

where $\boldsymbol{\theta}$ is the vector of unknown parameters. $\mathbf{Y} = \{\mathbf{y}_i^o, \mathbf{y}_i^m\}_{i=1}^n$ are the so-called *complete-data* which are the combination of observed and missing data. At the M-step, the parameters are updated by maximizing the expected complete-data loglikelihood. To summarize, if $\boldsymbol{\theta}^{(t)}$ is the current estimate of the parameter $\boldsymbol{\theta}$ and $f(\cdot)$ the density function, the E-step computes

$$Q(\boldsymbol{\theta}|\boldsymbol{\theta}^{(t)}) = \int \mathcal{L}_c(\boldsymbol{\theta}|\mathbf{Y}) f(\mathbf{y}^m|\mathbf{y}^o, \boldsymbol{\theta}^{(t)}) d\mathbf{y}^m \quad (8)$$

⁶Indeed, it is not the missing values themselves that are filled, but the function of the missing values (the sufficient statistics) that are computed [34].

and the M-step find $\boldsymbol{\theta}^{(t+1)}$ by maximizing (8):

$$Q(\boldsymbol{\theta}^{(t+1)}|\boldsymbol{\theta}^{(t)}) \geq Q(\boldsymbol{\theta}|\boldsymbol{\theta}^{(t)}) \quad (9)$$

The goal is then to repeat E and M-steps until a stopping criteria, such as the distance $\|\boldsymbol{\theta}^{(m+1)} - \boldsymbol{\theta}^{(m)}\|$, converges to a pre-defined threshold.

3. Covariance estimation under non-Gaussian environment

In this section, covariance matrix estimation procedures are developed in the presence of missing data under the CG distribution. The rank constraint given by (4) is also resolved. For both configurations, the EM algorithm is adopted. In the following, we consider the determinant-based normalization [44] which leads to the estimation of the normalized CM $\boldsymbol{\Sigma}/|\boldsymbol{\Sigma}|^{\frac{1}{p}}$, called the shape matrix.

3.1. Robust full-rank estimation

In this case, the unknown parameters to estimate are $\boldsymbol{\theta} = [\boldsymbol{\zeta}^\top, \{\tau_i\}_{i=1}^n]^\top$, where $\boldsymbol{\zeta}$ contains the elements of the lower triangular matrix of $\boldsymbol{\Sigma}$ including its diagonal. Following the expression of the likelihood function of the CG distribution (3), the complete-data loglikelihood is alternatively given by:

$$\mathcal{L}_c(\boldsymbol{\theta}|\mathbf{Y}) \propto -n \log |\boldsymbol{\Sigma}| - p \sum_{i=1}^n \log \tau_i - \sum_{i=1}^n \mathbf{y}_i^\top (\tau_i \boldsymbol{\Sigma})^{-1} \mathbf{y}_i \quad (10)$$

As we shall see hereafter, the differences with the purely Gaussian case ($\tau_i = 1$) are that 1) the unknown scales τ_i must be taken into account in the formulation and computation of the expectation at the E-step and 2) a closed-form expression $\hat{\tau}_i$ must be derived to update $\hat{\boldsymbol{\Sigma}}$ at the M-step.

Replacing \mathbf{y}_i by its permuted version $\tilde{\mathbf{y}}_i$, (10) can be written again as:

$$\mathcal{L}_c(\boldsymbol{\theta}|\mathbf{Y}) \propto -n \log |\boldsymbol{\Sigma}| - p \sum_{i=1}^n \log \tau_i - \sum_{i=1}^n \tilde{\mathbf{y}}_i^\top (\tau_i \tilde{\boldsymbol{\Sigma}})^{-1} \tilde{\mathbf{y}}_i$$

At the E-step of the algorithm, the expectation of the complete log-likelihood (11) is computed by using the so-called Q -function. This function is the expectation of the

missing data conditioned by the estimation of the parameters at the t -th iteration of the algorithm, that is:

$$Q_i(\boldsymbol{\theta}|\boldsymbol{\theta}^{(t)}) = \mathbb{E}_{\mathbf{y}_i^m|\mathbf{y}_i^o, \boldsymbol{\theta}^{(t)}} [\mathcal{L}_c(\boldsymbol{\theta}|\mathbf{y}_i^o, \mathbf{y}_i^m)] \quad (11)$$

The computation of (11) is hastened as both first and second terms of (11) are deterministic, which means that only the expectation of the last term has to be computed. Due to the iid of the observations, one obtains:

$$Q(\boldsymbol{\theta}|\boldsymbol{\theta}^{(t)}) = \sum_{i=1}^n Q_i(\boldsymbol{\theta}|\boldsymbol{\theta}^{(t)}) \quad (12)$$

where

$$\begin{aligned} Q_i(\boldsymbol{\theta}|\boldsymbol{\theta}^{(t)}) &= \mathbb{E}_{\mathbf{y}_i^m|\mathbf{y}_i^o, \boldsymbol{\theta}^{(t)}} \left[\tilde{\mathbf{y}}_i^\top (\tau_i \tilde{\boldsymbol{\Sigma}})^{-1} \tilde{\mathbf{y}}_i \right] \\ &= \mathbb{E}_{\mathbf{y}_i^m|\mathbf{y}_i^o, \boldsymbol{\theta}^{(t)}} \left[\begin{pmatrix} \mathbf{y}_i^o \\ \mathbf{y}_i^m \end{pmatrix}^\top (\tau_i \tilde{\boldsymbol{\Sigma}})^{-1} \begin{pmatrix} \mathbf{y}_i^o \\ \mathbf{y}_i^m \end{pmatrix} \right] \end{aligned}$$

To calculate each $Q_i(\boldsymbol{\theta}|\boldsymbol{\theta}^{(t)})$, the $\text{tr}\{\cdot\}$ function is used to develop the above expression:

$$\begin{aligned} Q_i(\boldsymbol{\theta}|\boldsymbol{\theta}^{(t)}) &= \mathbb{E}_{\mathbf{y}_i^m|\mathbf{y}_i^o, \boldsymbol{\theta}^{(t)}} \left[\text{tr} \left\{ \begin{pmatrix} \mathbf{y}_i^o \\ \mathbf{y}_i^m \end{pmatrix} \begin{pmatrix} \mathbf{y}_i^{o\top} & \mathbf{y}_i^{m\top} \end{pmatrix} (\tau_i \tilde{\boldsymbol{\Sigma}})^{-1} \right\} \right] \\ &= \tau_i^{-1} \text{tr} \left\{ \mathbb{E}_{\mathbf{y}_i^m|\mathbf{y}_i^o, \boldsymbol{\theta}^{(t)}} \left[\begin{pmatrix} \mathbf{y}_i^o \mathbf{y}_i^{o\top} & \mathbf{y}_i^o \mathbf{y}_i^{m\top} \\ \mathbf{y}_i^m \mathbf{y}_i^{o\top} & \mathbf{y}_i^m \mathbf{y}_i^{m\top} \end{pmatrix} \right] \tilde{\boldsymbol{\Sigma}}^{-1} \right\} \\ &= \tau_i^{-1} \text{tr} \{ \mathbf{B}_i^{(t)} \tilde{\boldsymbol{\Sigma}}^{-1} \} \quad (13) \end{aligned}$$

where $\mathbf{B}_i^{(t)} = \begin{pmatrix} \mathbf{D}^{(t)} & \mathbf{E}^{(t)} \\ \mathbf{F}^{(t)} & \mathbf{G}^{(t)} \end{pmatrix}$ is a $p \times p$ matrix at iteration t of the EM algorithm, with blocks given by

$$\mathbf{D}^{(t)} = \mathbb{E}_{\mathbf{y}_i^m|\mathbf{y}_i^o, \boldsymbol{\theta}^{(t)}} [\mathbf{y}_i^o \mathbf{y}_i^{o\top}] = \mathbf{y}_i^o \mathbf{y}_i^{o\top} \quad (14)$$

$$\mathbf{E}^{(t)} = \mathbf{F}^{(t)} = \mathbb{E}_{\mathbf{y}_i^m|\mathbf{y}_i^o, \boldsymbol{\theta}^{(t)}} [\mathbf{y}_i^m \mathbf{y}_i^{o\top}] = \mathbf{0} \quad (15)$$

$$\mathbf{G}^{(t)} = \mathbb{E}_{\mathbf{y}_i^m|\mathbf{y}_i^o, \boldsymbol{\theta}^{(t)}} [\mathbf{y}_i^m \mathbf{y}_i^{m\top}] \quad (16)$$

The only remaining expectation to compute is $\mathbf{G}^{(t)} = \mathbb{E}_{\mathbf{y}_i^m | \mathbf{y}_i^o, \boldsymbol{\theta}^{(t)}} [\mathbf{y}_i^m \mathbf{y}_i^{m\top}]$, which is the expectation of the missing data conditioned by the observed data. Here, the use of a classical result on conditional distributions (see Theorem 2.5.1 in [45], p. 35) gives the following expression:

$$\begin{aligned} \mathbb{E}_{\mathbf{y}_i^m | \mathbf{y}_i^o, \boldsymbol{\theta}^{(t)}} [\mathbf{y}_i^m \mathbf{y}_i^{m\top}] &= \tau_i^{(t)} (\tilde{\boldsymbol{\Sigma}}_{i,mm}^{(t)} - \tilde{\boldsymbol{\Sigma}}_{i,mo}^{(t)} \tilde{\boldsymbol{\Sigma}}_{i,oo}^{-1(t)} \tilde{\boldsymbol{\Sigma}}_{i,om}^{(t)}) \\ &\quad + \tilde{\boldsymbol{\mu}}_{i,m|o}^{(t)} \tilde{\boldsymbol{\mu}}_{i,m|o}^{\top(t)} \end{aligned} \quad (17)$$

where $\tilde{\boldsymbol{\Sigma}}_{i,mm}^{(t)} - \tilde{\boldsymbol{\Sigma}}_{i,mo}^{(t)} \tilde{\boldsymbol{\Sigma}}_{i,oo}^{-1(t)} \tilde{\boldsymbol{\Sigma}}_{i,om}^{(t)}$ and $\tilde{\boldsymbol{\mu}}_{i,m|o}^{(t)} = \tilde{\boldsymbol{\Sigma}}_{i,mo}^{(t)} \tilde{\boldsymbol{\Sigma}}_{i,oo}^{-1(t)} \tilde{\boldsymbol{y}}_i^o$ are respectively the CM and the mean of the conditional distribution of \mathbf{y}_i^m given \mathbf{y}_i^o . Finally, $\boldsymbol{\theta}^{(t+1)}$ is obtained at the M-step of the algorithm as the solution of the following maximization problem:

$$\begin{aligned} \max_{\boldsymbol{\theta}} \quad & Q_i(\boldsymbol{\theta} | \boldsymbol{\theta}^{(t)}) \\ \text{subject to} \quad & \boldsymbol{\Sigma} \succeq \mathbf{0} \\ & \tau_i > 0, \quad \forall i \end{aligned} \quad (18)$$

Proposition 3.1. *The MLE $\hat{\boldsymbol{\Sigma}}$ and $\hat{\tau}_i$ of problem (18) are given by the following closed-form expressions:*

$$\hat{\tau}_i = \frac{\text{tr}(\mathbf{B}_i^{(t)} \hat{\boldsymbol{\Sigma}}^{-1})}{p} \quad \text{for } i \in [1, n] \quad (19)$$

$$\hat{\boldsymbol{\Sigma}} = \frac{p}{n} \sum_{i=1}^n \frac{\mathbf{C}_i^{(t)\top}}{\text{tr}(\mathbf{C}_i^{(t)} \hat{\boldsymbol{\Sigma}}^{-1})} \triangleq \mathcal{H}(\hat{\boldsymbol{\Sigma}}) \quad (20)$$

with $\mathbf{C}_i^{(t)} = \mathbf{P}_i^\top \mathbf{B}_i^{(t)} \mathbf{P}_i$ and where $\mathcal{H}(\cdot)$ is the fixed point equation.

Proof. Let us first differentiate the complete-data loglikelihood \mathcal{L}_c in (11) w.r.t. τ_i and resolve the equality $\frac{\partial \mathcal{L}_c}{\partial \tau_i} = 0$, which is trivial and gives $\hat{\tau}_i = \frac{\text{tr}(\mathbf{B}_i^{(t)} \boldsymbol{\Sigma}^{-1})}{p}$.

By replacing τ_i by $\hat{\tau}_i$ in (11), we obtain the following loglikelihood:

$$\mathcal{L}_c = -n \log |\boldsymbol{\Sigma}| - p \sum_{i=1}^n \log \frac{\text{tr}(\mathbf{B}_i^{(t)} \tilde{\boldsymbol{\Sigma}}^{-1})}{p} - np$$

Then, we derive the loglikelihood w.r.t. to $\boldsymbol{\Sigma}$, which leads to the resolution of the following equation:

$$\frac{\delta \mathcal{L}_c}{\delta \Sigma} = 0$$

This first gives

$$-n\widehat{\Sigma}^{-1} - p \sum_{i=1}^n \frac{\widehat{\Sigma}^{-1} \mathbf{C}_i^{(t)\top} \widehat{\Sigma}^{-1}}{\text{tr}(\mathbf{C}_i^{(t)} \widehat{\Sigma}^{-1})} = 0$$

where $\mathbf{C}_i^{(t)} = \mathbf{P}_i^\top \mathbf{B}_i^{(t)} \mathbf{P}_i$. Arranging terms, then multiplying right and left terms by $\widehat{\Sigma}$ gives the desired closed-form expression. \square

Remark 2. For $n > p$, which is our case, this estimator can be computed using the fixed point algorithm $\Sigma^{(t+1)} = \mathcal{H}(\Sigma^{(t)})$ where m refers to the iteration index.

Remark 3. In the Gaussian case, finding Σ that maximizes this expression requires to derive Q with respect to Σ and then to solve $\frac{\partial Q}{\partial \Sigma} = 0$. Based on the above and after some basic derivation calculus, the solution to be computed at each iteration of the EM algorithm is given by:

$$\Sigma^{(t+1)} = \frac{1}{n} \mathbf{C}^{(t)\top} \quad (21)$$

with $\mathbf{C}^{(t)} = \sum_{i=1}^n \mathbf{P}_i^\top \mathbf{B}_i^{(t)} \mathbf{P}_i$. Finally, one can notice that in the case of no missing values, this result leads to the classical Sample Covariance Matrix (SCM) with $\mathbf{P}_i = \mathbf{I}_p$ and $\mathbf{B}_i = \mathbb{E}[\mathbf{y}_i \mathbf{y}_i^\top]$.

The complete estimation procedure of θ is given in Algorithm 1. The stopping condition of the EM algorithm is ensured by the evaluation of the quantity $\|\theta^{(t+1)} - \theta^{(t)}\|_F^2$ at each iteration, while the convergence of the fixed point algorithm relies on $\|\Sigma^{(m+1)} - \Sigma^{(m)}\|_F^2$. Note that the fixed point loop is optional as it can be seen as an inner EM where $\{\tau_i\}$ is the set of latent variables (hence a single update still increases the likelihood). Our empirical experiments evidenced that both versions of the algorithm achieve similar performance, while performing only a single fixed point iteration tends to achieve a faster convergence.

At the step $t = 0$, the estimate $\Sigma^{(0)}$ is initialized with Tyler's estimator from available observations in their full dimension p , denoted $\widehat{\Sigma}_{\text{Ty1-obs}}$. Unlike Σ , incomplete observations make the direct estimation of τ with the fixed point impracticable: thus, as an initialization, all $\tau_i^{(0)}$ are set to one.

Algorithm 1 EM-Tyl: Estimation of $\boldsymbol{\theta}$ under CG distribution with missing values.

Require: $\{\tilde{\mathbf{y}}_i\}_{i=1}^n \sim \mathcal{N}(\mathbf{0}, \tau_i \boldsymbol{\Sigma}), \{\mathbf{P}_i\}_{i=1}^n$

Ensure: $\hat{\boldsymbol{\Sigma}}, \hat{\tau}_i$

1: Initialization:

$$\begin{aligned}\boldsymbol{\Sigma}^{(0)} &= \hat{\boldsymbol{\Sigma}}_{\text{Tyl-obs}} \\ \boldsymbol{\tau}^{(0)} &= \mathbf{1}_N^\top\end{aligned}$$

2: **repeat**

▷ EM loop, t varies

3: Compute

$$\begin{aligned}\mathbf{G}^{(t)} &= \tau_i^{(t)} (\tilde{\boldsymbol{\Sigma}}_{i,mm}^{(t)} - \tilde{\boldsymbol{\Sigma}}_{i,mo}^{(t)} \tilde{\boldsymbol{\Sigma}}_{i,oo}^{-1(t)} \tilde{\boldsymbol{\Sigma}}_{i,om}^{(t)}) \\ &\quad + \tilde{\boldsymbol{\Sigma}}_{i,mo}^{(t)} \tilde{\boldsymbol{\Sigma}}_{i,oo}^{-1(t)} \tilde{\mathbf{y}}_i^o (\tilde{\boldsymbol{\Sigma}}_{i,mo}^{(t)} \tilde{\boldsymbol{\Sigma}}_{i,oo}^{-1(t)} \tilde{\mathbf{y}}_i^o)^\top\end{aligned}$$

4: Compute $\mathbf{B}_i^{(t)} = \begin{pmatrix} \mathbf{D}^{(t)} & \mathbf{0} \\ \mathbf{0} & \mathbf{G}^{(t)} \end{pmatrix}$ and $\mathbf{C}^{(t)}$

5: **repeat**

▷ fixed point, m varies (optional loop)

6: $\hat{\boldsymbol{\Sigma}}_{m+1}^{(t)} = \mathcal{H}(\hat{\boldsymbol{\Sigma}}_m^{(t)})$

7: **until** $\|\boldsymbol{\Sigma}^{(m+1)} - \boldsymbol{\Sigma}^{(m)}\|_F^2$ converges

8: Compute $\hat{\tau}_i^{(t)}, \quad i = 1, \dots, n$

9: $t \leftarrow t + 1$

10: **until** $\|\boldsymbol{\theta}^{(t+1)} - \boldsymbol{\theta}^{(t)}\|_F^2$ converges

3.2. Robust low-rank estimation

Let us now consider the case of data whose covariance matrix lives in a subspace of dimension $r < p$. As we recall, this configuration is useful in many real signal applications and is closely related to principal component analysis (PCA) and signal subspace estimation [42].

Following model (4), the parameters to estimate are now given by $\boldsymbol{\theta} = [\boldsymbol{\zeta}^\top, \sigma^2, \{\tau_i\}_{i=1}^n]^\top$, where $\boldsymbol{\zeta}$ contains the elements of the lower triangular matrix of \mathbf{H} . The maximization problem (18) to find $\boldsymbol{\theta}^{(t+1)}$ at the M-step of the EM algorithm becomes the following low-rank estimation problem:

$$\begin{aligned} \max_{\boldsymbol{\theta}} \quad & Q_i(\boldsymbol{\theta}|\boldsymbol{\theta}^{(t)}) \\ & \boldsymbol{\Sigma} = \sigma^2 \mathbf{I}_p + \mathbf{H} \\ \text{subject to} \quad & \text{rank}(\boldsymbol{\Sigma}) = r \\ & \sigma > 0, \quad \tau_i > 0, \quad \forall i \end{aligned} \tag{22}$$

A general solution to this problem was found in the seminal work of [42], which is recalled hereafter using the form given in [46] and [47]:

$$\widehat{\boldsymbol{\Sigma}} = \widehat{\sigma}^2 \mathbf{I}_p + \sum_{i=1}^r \widehat{\lambda}_i \mathbf{u}_i \mathbf{u}_i^\top \tag{23}$$

where

$$\widehat{\sigma}^2 = \frac{1}{p-r} \sum_{i=r+1}^p \lambda_i \tag{24}$$

$$\widehat{\lambda}_i = \lambda_i - \widehat{\sigma}^2, \quad i = 1, \dots, r \tag{25}$$

and $\boldsymbol{\Sigma} \stackrel{\text{EVD}}{=} \sum_{i=1}^p \lambda_i \mathbf{u}_i \mathbf{u}_i^\top$, where $\lambda_i < \dots < \lambda_p$ are the eigenvalues of $\boldsymbol{\Sigma}$ and \mathbf{u}_i the corresponding eigenvectors.

The procedure to estimate $\boldsymbol{\theta}$ under the LR assumption is given in Algorithm 2. It uses the same form than Algorithm 1 where equations (23)–(25) are applied just after the fixed point algorithm to each newly estimated $\boldsymbol{\Sigma}$. As stated in [47], the proof of convergence of the low-rank estimation algorithm is ensured by standard convergence results of the majorization-minimization (MM) algorithm [48]. Finally, the estimation of the scales $\boldsymbol{\tau}$ does not change from the former full-rank algorithm.

Algorithm 2 EM-Tyl-r: low-rank estimation of $\boldsymbol{\theta}$ under CG distribution with missing values.

Require: $\{\tilde{\mathbf{y}}_i\}_{i=1}^n \sim \mathcal{N}(\mathbf{0}, \tau_i \boldsymbol{\Sigma}), \{\mathbf{P}_i\}_{i=1}^n, \text{rank } r < p$

Ensure: $\hat{\boldsymbol{\Sigma}}, \{\hat{\tau}_i\}_{i=1}^n$

- 1: Initialize $\boldsymbol{\Sigma}^{(0)}, \boldsymbol{\tau}^{(0)}$ as in Algorithm 1.
 - 2: **repeat** ▷ EM loop, t varies
 - 3: Compute $\mathbf{G}^{(t)}, \mathbf{B}_i^{(t)}$ and $\mathbf{C}^{(t)}$
 - 4: **repeat** ▷ fixed point, m varies (optional loop)
 - 5: $\hat{\boldsymbol{\Sigma}}_{m+1}^{(t)} = \mathcal{H}(\hat{\boldsymbol{\Sigma}}_m^{(t)})$
 - 6: $\hat{\boldsymbol{\Sigma}}_{m+1}^{(t)} \stackrel{\text{EVD}}{=} \sum_{i=1}^p \lambda_i \mathbf{u}_i \mathbf{u}_i^\top$
 - 7: Update $\hat{\boldsymbol{\Sigma}}_{m+1}^{(t)}$ by computing (23), (24), (25)
 - 8: $\hat{\boldsymbol{\Sigma}}_{m+1}^{(t)} = \hat{\boldsymbol{\Sigma}}_{m+1}^{(t)} / \text{tr}(\hat{\boldsymbol{\Sigma}}_{m+1}^{(t)})$
 - 9: **until** $\|\boldsymbol{\Sigma}^{(m+1)} - \boldsymbol{\Sigma}^{(m)}\|_F^2$ converges
 - 10: Compute $\hat{\tau}_i^{(t)}, \quad i = 1, \dots, n$
 - 11: $t \leftarrow t + 1$
 - 12: **until** $\|\boldsymbol{\theta}^{(t+1)} - \boldsymbol{\theta}^{(t)}\|_F^2$ converges
-

4. Numerical simulations

This section illustrates the validation of the proposed algorithms with numerical experiments on simulated data drawn from the multivariate Gaussian and scaled Gaussian distributions. The performances of the proposed covariance estimation procedure are evaluated in regard to three aspects corresponding to different experiments:

- 1) The missing data ratio and patterns in subsection 4.1;
- 2) The quantity of outliers corrupting the data in subsection 4.2;
- 3) The possibility to perform CM-based data imputation in the presence of outliers and missing data in subsection 4.3.

For the sake of the experiment, the CM and scales parameters are known. The CM is chosen to be Toeplitz⁷ which has the form:

$$(\mathbf{R})_{ij} = \rho^{|i-j|} \quad (26)$$

Parameter ρ , which controls the correlation structure of the CM, is set to 0.65. Scales $\{\tau_i\}_{i=1}^n$ are drawn from a Gamma distribution with shape parameter α and scale parameter $\beta = \frac{1}{\alpha}$. In all experiments, we fix $\alpha = 1$. To generate a covariance matrix admitting the structure (4), we compute:

$$\mathbf{\Sigma} = \mathbf{I}_p + \sigma^2 \mathbf{U} \mathbf{U}^\top \quad (27)$$

where $\mathbf{U} \in \text{St}_{p,r}$ is the underlying signal subspace basis obtained from the eigenvalue decomposition of \mathbf{R} and σ is a free parameter corresponding to the signal to noise ratio.

In our experiments, the data dimension is $p = 15$ and $n = \{63, 109, 190, 331, 575, 1000\}$. Sets $\{\mathbf{y}_i\}_{i=1}^n$ are drawn from the scaled Gaussian distribution with covariance $\mathbf{\Sigma}$. As the aim is to estimate the structured covariance matrix $\mathbf{\Sigma}$, the estimation is performed on 500 (or 200 depending on the experiment) sets $\{\mathbf{y}_i\}_{i=1}^n$ simulated for each value of n . Indeed, for the sake of the experiment, missing data are also simulated, which allows a

⁷Note that this information on the structure is not used in the estimation procedure.

full control on their ratio and pattern. Importantly, as n increases from 63 to 1000, the missing data ratio decreases as {44, 22, 11, 5, 2, 1}%.

The following covariance estimators are considered for comparison:

i) Covariance matrix obtained from algorithm 1 for Gaussian and CG distributions and their LR version from algorithm 2, respectively named $\widehat{\Sigma}_{\text{EM-SCM}}$, $\widehat{\Sigma}_{\text{EM-Tyl}}$, $\widehat{\Sigma}_{\text{EM-SCM-r}}$ and $\widehat{\Sigma}_{\text{EM-Tyl-r}}$.

ii) *Sample covariance matrix* (SCM) from the clairvoyant data (without missing data):

$$\widehat{\Sigma}_{\text{SCM-clair}} = \frac{1}{n} \sum_{i=1}^n \mathbf{y}_i \mathbf{y}_i^\top \quad (28)$$

iii) The SCM $\widehat{\Sigma}_{\text{SCM-obs}}$ estimated from observed vectors only, that is $\mathbf{y}_i = \mathbf{y}_i^o$ with $i \in [1, n]$.

iv) The *fixed point* estimator or Tyler's estimator from the clairvoyant data:

$$\widehat{\Sigma}_{\text{Tyl-clair}} = \frac{p}{n} \sum_{i=1}^n \frac{\mathbf{y}_i \mathbf{y}_i^\top}{\mathbf{y}_i \Sigma^{-1} \mathbf{y}_i^\top} \quad (29)$$

v) Tyler's estimator $\widehat{\Sigma}_{\text{Tyl-obs}}$ from observed vectors, that is $\mathbf{y}_i = \mathbf{y}_i^o$ with $i \in [1, n]$.

vi) Multiple imputation (MI) [49, 6] from which a robust version is proposed (RMI): q imputed data sets $(\mathbf{Y}_1, \mathbf{Y}_2, \dots, \mathbf{Y}_q)$ are generated with missing elements drawn from a CG distribution:

$$\widehat{\mathbf{y}}_{ij}^m \sim \mathcal{N}(\boldsymbol{\mu}_{ij}^o, \sqrt{\tau_{ij}} \boldsymbol{\sigma}_{ij}^o), \quad j = 1, \dots, q \quad (30)$$

where $\boldsymbol{\mu}_{ij}^o$ and $\boldsymbol{\sigma}_{ij}^o$ are the mean and variance of the observed components of \mathbf{y}_{ij} , and τ_{ij} are the scales parameters drawn from the Gamma distribution with shape parameter $\alpha = 1$. The estimated covariance is the mean of the q Tyler's estimators from the q imputed data sets:

$$\widehat{\Sigma}_{\text{RMI}} = \frac{1}{q} \sum_{j=1}^q \Sigma_{\text{Tyl},j} = \frac{p}{nq} \sum_{j=1}^q \sum_{i=1}^n \frac{\mathbf{y}_{ij} \mathbf{y}_{ij}^\top}{\mathbf{y}_{ij} \Sigma_j^{-1} \mathbf{y}_{ij}^\top} \quad (31)$$

vii) Robust stochastic imputation (RSI): this procedure is the same than MI, but with $q = 1$.

viii) Mean imputation [6]: missing components of each vector \mathbf{y}_i are imputed by the mean of the observed components:

$$\widehat{\mathbf{y}}_i^m = \boldsymbol{\mu}_i^o \quad (32)$$

Then, the covariance $\widehat{\boldsymbol{\Sigma}}_{\text{Mean-Tyl}}$ is estimated using Tyler's estimator.

4.1. Covariance estimation with missing data

This experiment shows the performances of covariance estimation as functions of the missing data ratio and missing data patterns. To compare the estimated covariance matrix to the true data covariance, the following geodesic distance is used [50]:

$$\delta_{\mathcal{S}_{++}^p}^2(\boldsymbol{\Sigma}, \widehat{\boldsymbol{\Sigma}}) = \|\log(\boldsymbol{\Sigma}^{-\frac{1}{2}} \widehat{\boldsymbol{\Sigma}} \boldsymbol{\Sigma}^{-\frac{1}{2}})\|_2^2 \quad (33)$$

This distance, which is sufficient to measure estimation errors, emanates from the Fisher metric for the Gaussian distribution on \mathcal{S}_{++}^p [51].

Three missing data patterns are examined, which correspond to the following configurations (see Fig. 1):

- One block of missing data of size (7×20) . This is a special case of the monotone missing data pattern as studied in [12, 20]. This configuration corresponds to the case where one group of variables is missing at the same observations, e.g. a group of sensors that are equally interrupted in time. This case is referred to as *monotone pattern* in the experiments.
- Multiple blocks of missing data with various size and randomly scattered into the data set. This configuration corresponds to the general missing data pattern. It is most likely to happen in real-life applications (see, e.g. [52, 8]). This case is referred to as *general pattern*.
- Randomly distributed missing data. This configuration is also a general missing data pattern except that multiple values for one variable at one observation are missing across the dataset. This case is referred to as *random pattern*.

Fig. 3 and 4 show the results in terms of mean distance for two rank settings (the full rank case $r = p$ and the low-rank case with $r = 5$) and the three aforementioned pattern

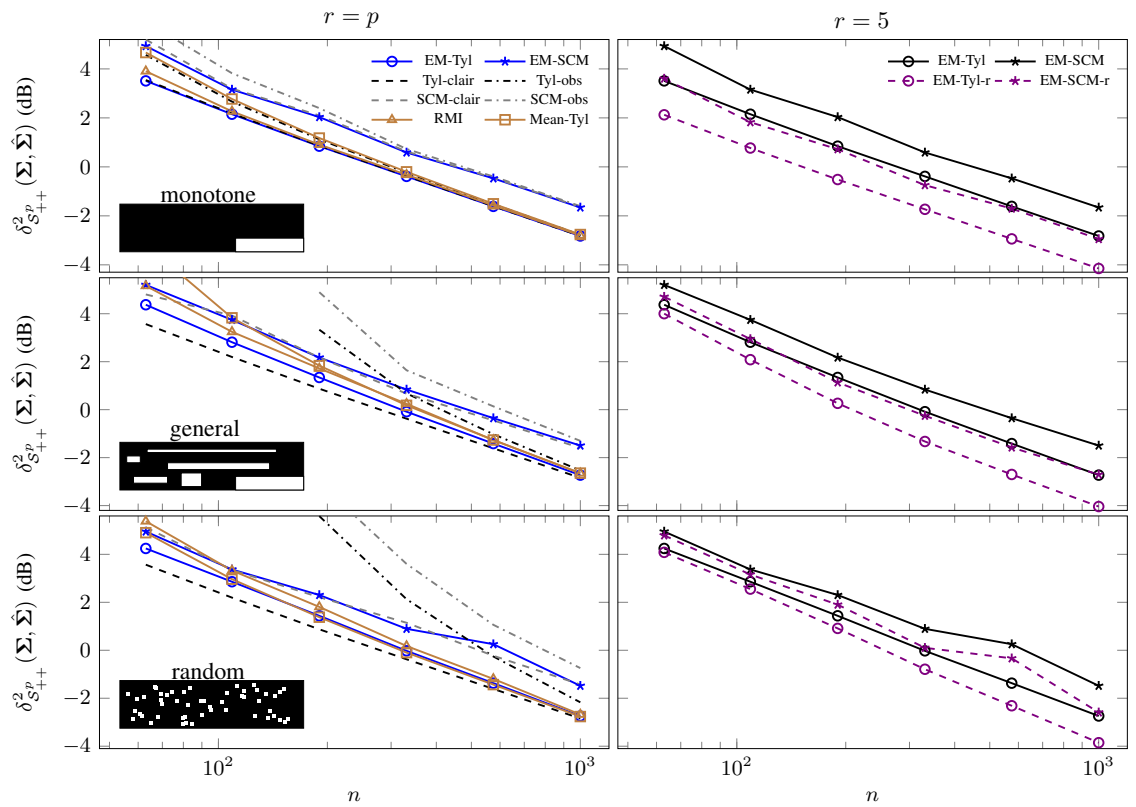


Figure 3: Mean of error measures 33 for $r = p$ (left) and $r = 5$ (right) of methods EM-Tyl, EM-Tyl-r, EM-SCM, EM-SCM-r, Tyl-clair, Tyl-obs, SCM-clair, SCM-obs, RMI and mean imputation as functions of the number of samples n . The mean are computed over 500 simulated sets $\{\mathbf{y}_i\}_{i=1}^n$ for monotone (top), general (middle) and random (bottom) missing data pattern with $p = 15$.

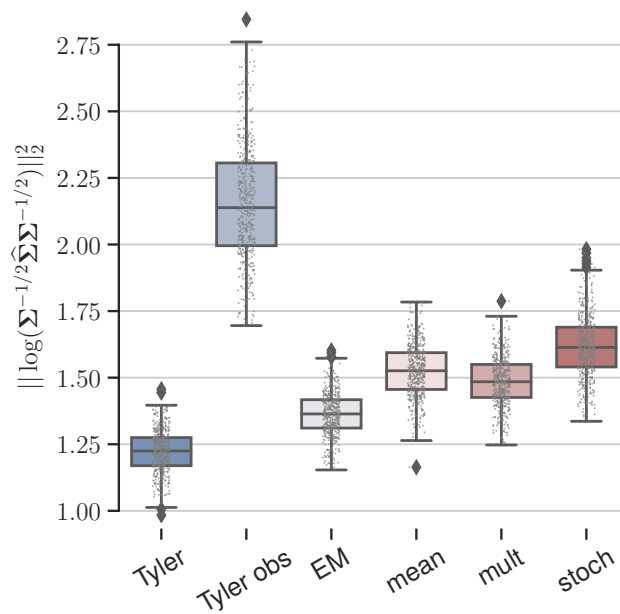


Figure 4: Boxplots showing geodesic distances of Tyler, Tyler observed, EM (ours), mean imputation, multiple imputation and stochastic imputation methods for $r = p$ and $n = 200$. Small dots show the computed distances over 500 simulated sets $\{\mathbf{y}_i\}_{i=1}^n$ corrupted by 20% of missing data with general pattern, which corresponds to the middle-left plot of Fig. 3.

configurations. In the full rank case, EM-Tyl shows better performances than all other estimators. For the random pattern configuration, this result stands for regular sample size but not when n increases where EM-Tyl exhibits similar errors than mean imputation. Good performances of the latter can be explained by the increasing availability of observations as n increases, which gives a better estimate of $\boldsymbol{\mu}_i^o$. Unsurprisingly, all estimators (except the ones based on the SCM) reach Tyler’s estimator as the missing data ratio decreases for large sample size. In the case of Gaussian estimators, the EM-SCM shows very close performances than the clairvoyant SCM. As expected, Tyl-obs and SCM-obs display poor performances when the missing data ratio increases. The advantage of the low-rank model is illustrated for $r = 5$, where LR estimators systematically display lower errors than the full-rank estimates.

4.2. Should outliers be discarded?

Data corrupted by outliers is one of the main motivation of robust estimation [53]. In this case, one can be interested to know whether Tyler’s estimator or EM-Tyl estimator gives higher performances. In the complete data case, the former can be directly estimated with outliers. To estimate the latter, outliers can be discarded or masked (i.e. set as missing data) if their position are known, which is a common approach in various applications. In the following, a data set $\{\mathbf{y}_i\}_{i=1}^n$ is drawn from the CG distribution with a fixed number of samples $n = 200$. Outliers are generated by adding white Gaussian noise (WGN) $\mathbf{z}_i \sim \mathcal{N}(\mathbf{0}, \sigma_{wgn})$ with an increasing variance σ_{wgn} on randomly selected observations \mathbf{y}_i .

Three data sets are considered to compare the CM estimation errors:

- 1) Corrupted data $\mathbf{y}_i + \mathbf{z}_i$;
- 2) Masked data where the outliers are set as missing data.
- 3) Data without outliers \mathbf{y}_i ;

Tyler’s estimator is computed on data set 1), whereas the EM-Tyl algorithm is applied to data set 2). Finally, the clairvoyant SCM and Tyler’s estimators are computed from data set 3).

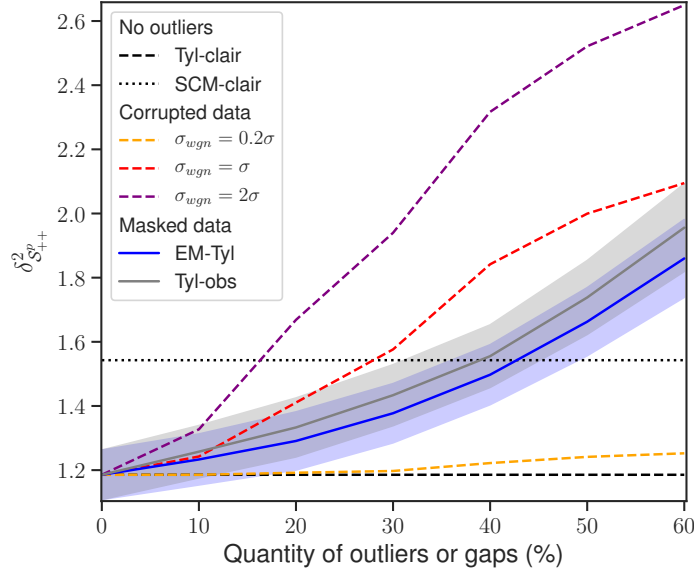


Figure 5: Mean geodesic distances over 200 simulated sets $\{\mathbf{y}_i\}_{i=1}^n$ as function of the missing data or outlier ratio (%) for $n = 200$. Tyl-clair and SCM-clair errors are shown with no outliers. Tyl-clair is displayed on corrupted data with different outlier variance σ_{wgn} w.r.t. the data variance σ . EM-Tyl and Tyl-obs errors are shown when outliers are masked as missing values.

Fig. 5 gives an overlook on what choice of the CM estimation procedure would be preferable. It shows that it mainly depends on the outlier variance: for a small σ_{wgn} , Tyler’s estimator should be preferred, whereas EM-Tyl is more suitable when the outlier variance reaches the variance of the signal σ . Note also that EM-Tyl provides better performances than the clairvoyant SCM until the missing data ratio reaches $\sim 45\%$ of the data.

4.3. Robust imputation of missing values with outliers

In this experiment, we propose to apply our estimators to missing data imputation with possible outliers corrupting the data. Missing data imputation [6] concerns a wide range of applications, including remote sensing [8]. A recent procedure to deal with missing values was developed, namely the EM-EOF method [54], which uses the EM algorithm and empirical orthogonal functions (EOFs) to iteratively decompose the CM and reconstruct the incomplete data with a few number of selected EOFs $k \ll p$. The final number of components is the one giving the minimal error between the initial data

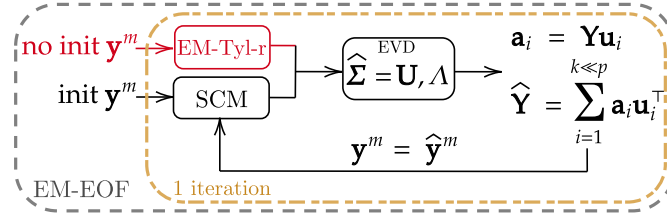


Figure 6: Diagram of the EM-EOF method [54] for missing data imputation. After initializing the missing values, the CM matrix is estimated from the data \mathbf{Y} , which is then reconstructed with a number of components $k \ll p$. Instead of using the SCM, the EM-Tyl-r estimator with $r = k$ is plugged in at the last iteration of the algorithm (in red).

and the imputed data. As shown in Fig. 6, instead of the SCM (which is used in the aforementioned study), the EM-Tyl-r estimator is used with $r = k$ at the last iteration of the EM-EOF algorithm. This is justified by the fact that this algorithm iteratively updates the SCM with the predicted missing values at each step, whereas the EM-Tyl-r estimator only needs the missing data pattern, which remains the same at each iteration. The RMI estimator (31) is also considered for comparison.

The data is generated using a Haystack-type model [55] which draws samples $\{\mathbf{y}_i\}_{i=1}^n$ as inliers \mathbf{y}_i^{in} and outliers $\mathbf{y}_i^{\text{out}}$:

$$\{\mathbf{y}_i\}_{i=1}^n = \{\{\mathbf{y}_i^{\text{in}}\}_{i \in \{1, \dots, n_{\text{in}}\}}, \{\mathbf{y}_i^{\text{out}}\}_{i \in \{1, \dots, n_{\text{out}}\}}\} \quad (34)$$

$$\mathbf{y}_i^{\text{in}} \sim \mathcal{N}(\mathbf{0}, \mathbf{I}_p + \sigma_s^2 \mathbf{U} \mathbf{U}^\top) \quad (35)$$

$$\mathbf{y}_i^{\text{out}} \sim \mathcal{N}(\mathbf{0}, \mathbf{I}_p + \sigma_o^2 \mathbf{U}_\perp \mathbf{U}_\perp^\top) \quad (36)$$

where $\mathbf{U} \subset \text{St}_{p,k}$ is the signal subspace basis, σ_s^2 and σ_o^2 are respectively the signal to noise ratio (SNR) and the outlier to noise ratio (ONR), and $100 \times \frac{(n - n_{\text{in}})}{n}$ is the outlier ratio in the data set in percentage.

In the experiments, we choose $\sigma_s^2 = 10$, $\sigma_o^2 \in \{0, 1.5, 3, \dots, 30\}$ and the outlier ratio varies from 0 to 50% of the data. Note that inliers and outliers are whole vectors (not just entries) which are randomly chosen in the data set. 30% of the data is discarded as missing values under a general pattern.

To measure the performance of imputation, we compute the root-mean-square error (RMSE) between a cross-validation (CV) data set $\mathcal{Y} = \{y_1, y_2, \dots, y_s\} \in \mathbf{Y}$ and its reconstruction $\hat{\mathcal{Y}}$ after imputation:

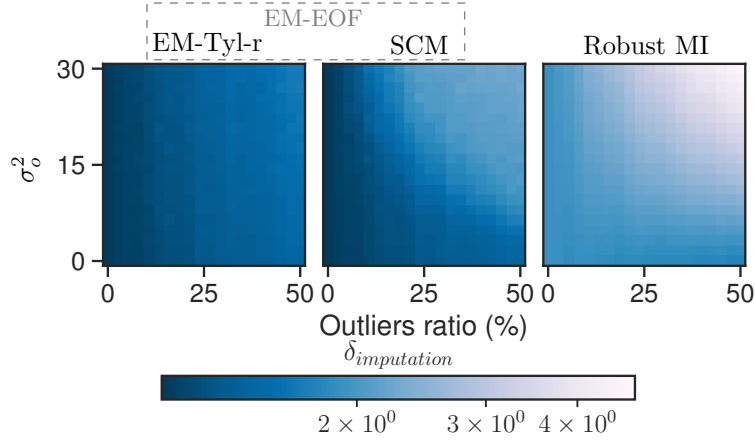


Figure 7: Mean of cross-validation error (37) over 200 simulated sets $\{\mathbf{y}_i\}_{i=1}^n$ as function of the outlier ratio (%) and signal to outlier ratio σ_o^2 for the EM-EOF using EM-Tyl-r estimator, EM-EOF using the SCM and RMI procedures. 30 % of missing data under the general pattern are generated. Chosen parameters are $n = 200$ and $p = 15$.

$$\delta_{imputation} = \left[\frac{1}{s} \sum_{i=1}^s |\hat{y}_s - y_s|^2 \right]^{1/2} \quad (37)$$

In total, 1% of the data is chosen for the cross-validation data set. These values are artificially removed and copied before the process, and compared to the new values after the imputation procedure. For model (34), CV errors illustrated by Fig. 7 show a substantial gain by replacing the SCM by the EM-Tyl-r estimator at the last step of the EM-EOF method, whereas RMI performs poorly. The gain is larger for important signal to outlier ratio σ_o^2 , which confirms the robustness of the proposed estimator for robust low-rank imputation under model (34).

5. Application to classification and clustering problems

5.1. Classification with missing values

In remote sensing, and more particularly in multispectral and hyperspectral imaging, missing data can arise for various reasons including:

- 1) Clouds when the sensor operates in the visible part of the spectrum [8];

- 2) Sensor failure, as the known problem on the scan-line corrector images of the Landsat ETM+ sensor [56] or Aqua MODIS band 6 [57];

In these cases, the data (or the entire band itself) is masked, downsampled to avoid temporal gaps or restored using specific gap-filling methods [56, 57]. When it comes to classification tasks, incomplete data is a challenge. In this scope, existing approaches classify, mask, and interpolate values from cloudy observations in a pre-processing step [58].

To tackle this challenge, the proposed estimators are used as a set of descriptors⁸ $\{\theta_i\}$ to a classification problem on the *BreizhCrops* data set [58]. The data consists of Sentinel-2 multivariate time series of field crop reflectances on the Brittany region over 23 spectral bands. It is divided into four sub-regions called FRH01, FRH02, FRH03 and FRH04 corresponding to the four departments of Brittany. These sub-regions contain field labels which are gathered in 9 selected classes representing crop categories, e.g. *barley, nuts, wheat*, etc. Following [58], each band is mean-aggregated over one field parcel to a feature vector $\mathbf{y}^t \in \mathbb{R}^p$, where p is the number of features (here the spectral bands) and t a timestamp. Thus, the whole data set is denoted $\{\{\mathbf{y}_k^t\}_{k=1}^K\}_{t=1}^T$, which corresponds to the aggregation of all reflectances at field parcels $k \in [1, K]$ and timestamps $t \in [1, T]$. The experiment is done on the L1C top-of-atmosphere product and on 13 bands selected by the *BreizhCrops* processing chain [58].

A supervised covariance-based classification is performed using a Riemannian minimum distance to riemannian mean (MDRM) classifier [59], which works in a test-training form. The training step provides a set of $p \times p$ SPD matrices encoding field parcels for the available classes. Assuming that the data is complete, the set of SCMs would be computed as:

$$\Sigma_k = \frac{1}{T} \sum_{t=1}^T \mathbf{y}_k^t (\mathbf{y}_k^t)^\top, \quad k = 1, \dots, K \quad (38)$$

For each class, a center of mass of the available parcels is estimated. In the test step, a field parcel is also encoded as an SPD matrix and then assigned to the class whose

⁸In machine learning problems, statistical descriptors are classically used as they are often more discriminative than raw data.

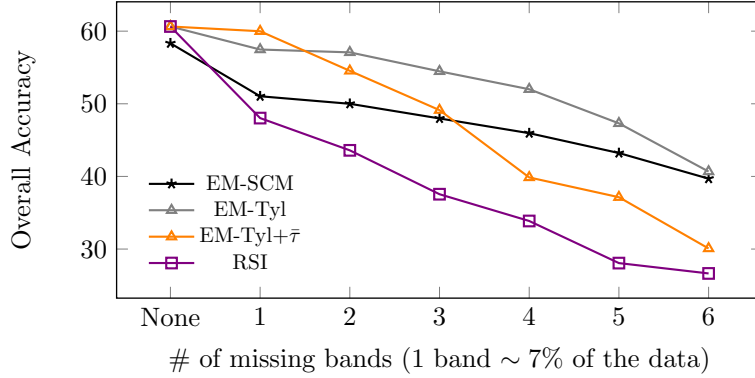


Figure 8: Classification mean overall accuracy (%) versus the number of randomly missing bands over 10 run of RMDM [60] classifier based on EM-SCM, EM-Tyl, EM-Tyl+ $\bar{\tau}$ and RSI estimators.

center of mass is the closest according to the distance (33) acting on the manifold \mathcal{S}_{++}^p [60].

Before the experiment, missing data are artificially created in the data set. For this, successive bands are set as missing and the performances are evaluated as function of the missing data ratio. The classifier is trained on the FRH04 region, whereas the test is done on FRH03.

Results in terms of overall accuracy (OA) for the FRH03 region versus the number of missing bands are displayed in Fig. 8, with EM-SCM, EM-Tyl and RSI estimators. A fourth estimator is added, named EM-Tyl+ $\bar{\tau}$, which corresponds to the EM-Tyl multiplied by the mean of the estimated scales $\hat{\tau}_i$ to add a power information to the estimator. Unfortunately, experiments have shown that the LR structure does not improve the OA, which might be due to the mean-aggregation over each parcel, which essentially acts as a filter.

Results show that, for this data set, the EM-Tyl-based classifier is more robust to missing bands than the EM-SCM one, whereas the RSI-based classifier gives a rapidly decreasing OA when the gaps ratio increases. The EM-Tyl+ $\bar{\tau}$ achieves good results for low missing data ratio but loses its efficiency when more bands are missing, which lowers the estimation accuracy of the mean of τ_i . Interestingly, for both EM-SCM and EM-Tyl, the OA is almost stable until the gap ratio reaches 21% of the data (3 missing bands).

5.2. Image clustering with missing values

We apply the proposed CM estimators to a hyperspectral image clustering problem using the *K-means++* algorithm [61] on the *Indian Pines* data set [62], consisting of a 145×145 pixels image with $p = 200$ bands. As in the classification problem, the proposed estimators EM-SCM and EM-Tyl are used as descriptors $\{\theta_i\}$, as well as EM-SCM-r and EM-Tyl-r. The aim is to partition the descriptors in a number of clusters which correspond to the 16 classes dividing the *Indian Pines* image.

The image is first centered by subtracting the global mean. Then, a sliding window of size $w \times w$ is applied to the image. One descriptor $\{\theta_i\}$ is estimated using the $n = w^2$ observations in each window denoted $\mathbf{X}_i \in \mathbb{R}^{p \times n}$. Thus, we obtain a set of descriptors $\{\theta_i\}$ to cluster using a *K-means++* [20]. For the descriptors using the low-rank model (4), the first $r = 5$ components are kept which concur with the five principal eigenvectors of the SCM of *Indian Pines* containing more than 95% of the total cumulative variance⁹.

Due to the high dimensionality and a possible runtime overflow due to the creation of missing data, the image is subsampled regularly to reduce the dimension to 20 bands and cropped to get a final 85×70 image composed by 5 or the 16 original classes (see Fig. 9a). As shown by Fig. 9b, sensor failure is simulated by adding missing values on random columns of selected bands.

The averaged Overall Accuracy (OA) are reported with their standard deviations (std) in Fig. 10. We observe that in general, the descriptors based on RSI and RSI-r estimators give lower accuracies compared to the descriptors using the SCM, SCM-r, EM-Tyl and EM-Tyl-r estimators. As the missing data ratio increases, EM-SCM give decreasing performances compared to the EM-Tyl which is stable. For large missing data ratio, EM-SCM-r performs surprisingly well compared to EM-Tyl and EM-Tyl-r. For lower missing data ratios, clustering achieves its best performances using the EM-Tyl-r estimator.

6. Conclusion

This article proposes a novel procedure based on the EM algorithm to perform robust low-rank estimation of the covariance matrix with missing data following a general

⁹This measure can be easily computed by the formula $\sum_{i=1}^r \lambda_i / \sum_{i=1}^p \lambda_i$.

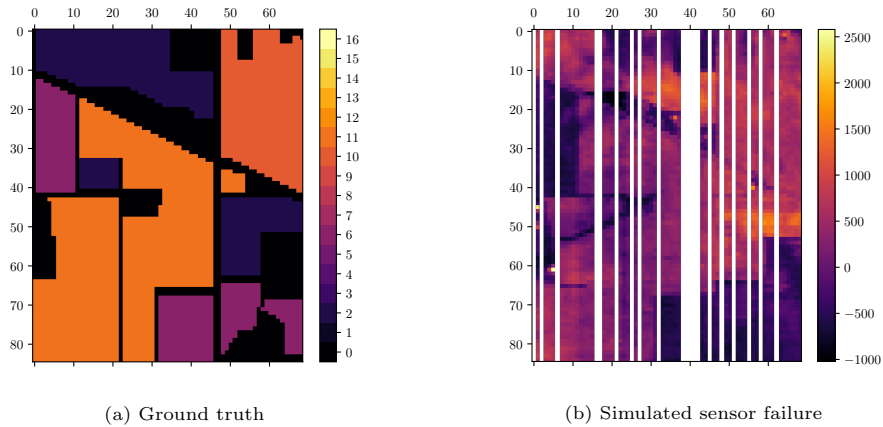


Figure 9: Selected sub-image of *Indian Pines*: ground truth (left) and simulated sensor failure on band 10 (right) where white stripes are the missing values (20 columns of pixels are set as missing).

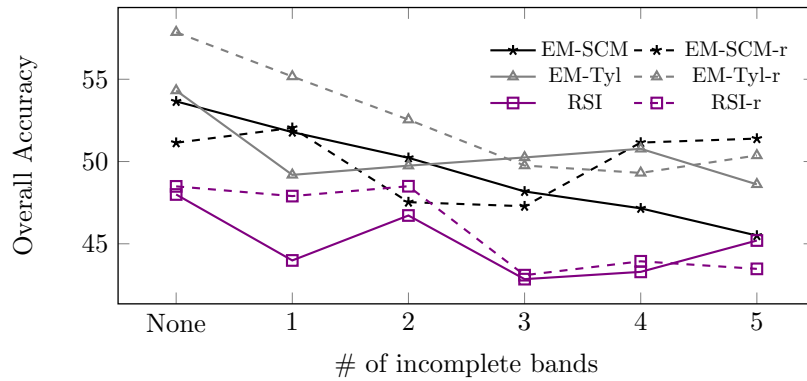


Figure 10: Clustering mean overall accuracy (%) versus the number of incomplete bands (as in Fig. 9b) over 10 run of the *Kmeans++* algorithm for the descriptors based on EM-SCM, EM-Tyl, RSI, EM-SCM-r, EM-Tyl-r and RSI-r estimators.

pattern. The developed tools take advantage of the CG distribution and of the LR structure of the covariance matrix. Closed-form expressions of the unknown CM and associated scales are derived and integrated to the M-step of the algorithm, which generalizes the Gaussian case. The performance of the proposed estimators are validated on simulated data sets with missing values and corrupted by outliers, as well as real-world incomplete data sets. Compared to the classical Gaussian assumption and to the unstructured model, experiments show the possibility to improve the results in terms of CM estimation and robust imputation, as well as supervised (classification) and unsupervised (image clustering) problems. Some potential extensions of this work include the extension to other classes of CG distributions and experimenting classification tasks with temporal gaps rather than spectral gaps, as well as more spectral information by reducing the downsampling rate.

Acknowledgment

The authors would like to thank Antoine Collas and Ammar Mian for their precious help to better understand the MDRM method and the *Kmeans++* algorithm, and Florent Bouchard for his deep insights in robust estimation and covariance-based classification and clustering.

References

- [1] T. W. Anderson, Maximum likelihood estimates for a multivariate normal distribution when some observations are missing, *Journal of the American Statistical Association* 52 (278) (1957) 200–203.
- [2] A. A. Afifi, R. M. Elashoff, Missing observations in multivariate statistics I. Review of the literature, *Journal of the American Statistical Association* 61 (315) (1966) 595–604.
- [3] R. J. A. Little, D. B. Rubin, *Statistical analysis with Missing Data*, Wiley, New York, 1987.
- [4] J. L. Schafer, *Analysis of incomplete multivariate data*, CRC press, 1997.
- [5] J.-P. Benzécri, et al., *L’analyse des données*, Vol. 2, Dunod Paris, 1973.
- [6] S. Van Buuren, *Flexible imputation of missing data*, CRC press, 2018.
- [7] B. Walczak, D. L. Massart, Dealing with missing data : Part I, *Chemom. Intell. Lab. Syst.* 58 (2001) 15–27.
- [8] H. Shen, X. Li, Q. Chen, C. Zeng, G. Yang, H. Li, L. Zhang, Missing information reconstruction of remote sensing data: A technical review, *IEEE Geosci. Remote Sens. Mag.* 3 (2015) 61–85. doi:10.1109/MGRS.2015.2441912.
- [9] D. B. Rubin, Inference and missing data, *Biometrika* 63 (3) (1976) 581–592.

- [10] A. P. Dempster, N. M. Laird, D. B. Rubin, Maximum likelihood from incomplete data via the EM algorithm, *J. Royal Statistical Society. Series B (Methodological)* 39 (1) (1977) 1–38.
- [11] M. Jamshidian, An EM algorithm for ML factor analysis with missing data, in: *Latent variable modeling and applications to causality*, Springer, 1997, pp. 247–258.
- [12] C. Liu, Efficient ML estimation of the multivariate normal distribution from incomplete data, *Journal of Multivariate Analysis* 69 (1999) 206–217. doi:10.1006/jmva.1998.1793.
- [13] T. Schneider, Analysis of incomplete climate data: Estimation of mean values and covariance matrices and imputation of missing values, *J. Climate* 14 (2001) 853–871.
- [14] K. Lounici, et al., High-dimensional covariance matrix estimation with missing observations, *Bernoulli* 20 (3) (2014) 1029–1058.
- [15] N. Städler, D. J. Stekhoven, P. Bühlmann, Pattern alternating maximization algorithm for missing data in high-dimensional problems., *J. Mach. Learn. Res.* 15 (1) (2014) 1903–1928.
- [16] T. Chen, E. Martin, G. Montague, Robust probabilistic PCA with missing data and contribution analysis for outlier detection, *Computational Statistics & Data Analysis* 53 (10) (2009) 3706–3716.
- [17] J. Josse, F. Husson, Handling missing values in exploratory multivariate data analysis methods, *Journal de la Société Française de Statistique* 153 (2) (2012) 79–99.
- [18] R. J. Little, Robust estimation of the mean and covariance matrix from data with missing values, *Journal of the Royal Statistical Society: Series C (Applied Statistics)* 37 (1) (1988) 23–38.
- [19] C. Liu, D. B. Rubin, ML estimation of the t distribution using EM and its extensions, ECM and ECME, *Statistica Sinica* (1995) 19–39.
- [20] J. Liu, D. P. Palomar, Regularized robust estimation of mean and covariance matrix for incomplete data, *Signal Processing* 165 (2019) 278 – 291. doi:https://doi.org/10.1016/j.sigpro.2019.07.009.
- [21] D. E. Tyler, A distribution-free M-estimator of multivariate scatter, *The Annals of Statistics* 15 (1) (1987) 234–251.
- [22] E. Conte, A. De Maio, G. Ricci, Recursive estimation of the covariance matrix of a compound-Gaussian process and its application to adaptive CFAR detection, *IEEE Transactions on signal processing* 50 (8) (2002) 1908–1915.
- [23] F. Pascal, Y. Chitour, J.-P. Ovarlez, P. Forster, P. Larzabal, Covariance structure maximum-likelihood estimates in compound Gaussian noise: Existence and algorithm analysis, *IEEE Transactions on Signal Processing* 56 (1) (2008) 34–48. doi:10.1109/TSP.2007.901652.
- [24] A. M. Zoubir, V. Koivunen, E. Ollila, M. Muma, *Robust statistics for signal processing*, Cambridge University Press, 2018.
- [25] F. Gini, M. V. Greco, M. Diani, L. Verrazzani, Performance analysis of two adaptive radar detectors against non-gaussian real sea clutter data, *IEEE Transactions on Aerospace and Electronic Systems* 36 (4) (2000) 1429–1439.
- [26] M. S. Greco, F. Gini, Statistical analysis of high-resolution SAR ground clutter data, *IEEE Transactions on Geoscience and Remote sensing* 45 (3) (2007) 566–575.
- [27] J. Theiler, B. Foy, A. Fraser, Characterizing non-gaussian clutter and detecting weak gaseous plumes

- in hyperspectral imagery, *Proceedings SPIE* 5806 (2005) 182–193.
- [28] P. Formont, F. Pascal, G. Vasile, J.-P. Ovarlez, L. Ferro-Famil, Statistical classification for heterogeneous polarimetric SAR images, *IEEE Journal of selected topics in Signal Processing* 5 (3) (2010) 567–576.
- [29] E. Ollila, D. E. Tyler, V. Koivunen, H. V. Poor, Complex elliptically symmetric distributions: Survey, new results and applications, *IEEE Transactions on signal processing* 60 (11) (2012) 5597–5625.
- [30] A. Mian, G. Ginolhac, J.-P. Ovarlez, A. M. Atto, New robust statistics for change detection in time series of multivariate SAR images, *IEEE Transactions on Signal Processing* 67 (2) (2018) 520–534.
- [31] G. Frahm, U. Jaekel, A generalization of Tyler’s M-estimators to the case of incomplete data, *Computational Statistics & Data Analysis* 54 (2) (2010) 374–393.
- [32] R. J. Little, D. B. Rubin, *Statistical analysis with missing data*, Vol. 793, John Wiley & Sons, 2019.
- [33] E. G. Larsson, P. Stoica, High-resolution direction finding: the missing data case, *IEEE transactions on signal processing* 49 (5) (2001) 950–958.
- [34] R. J. A. Little, D. B. Rubin, *Statistical analysis with Missing Data*, 2nd Edition, Wiley, New York, 2002.
- [35] N. Goodman, J. Stiles, On clutter rank observed by arbitrary arrays., *IEEE Transactions on Signal Processing* 55 (2007) 178–186.
- [36] K. Yao, A representation theorem and its applications to spherically-invariant random processes, *IEEE Transactions on Information Theory* 19 (5) (1973) 600–608.
- [37] R. A. Maronna, R. D. Martin, V. J. Yohai, M. Salibián-Barrera, *Robust statistics: theory and methods (with R)*, John Wiley & Sons, 2019.
- [38] A. Wiesel, Unified framework to regularized covariance estimation in scaled Gaussian models, *IEEE Transactions on Signal Processing* 60 (1) (2012) 29–38. doi:10.1109/TSP.2011.2170685.
- [39] D. Ruppert, D. S. Matteson, *Statistics and data analysis for financial engineering*, Vol. 13, Springer, 2011.
- [40] I. M. Johnstone, On the distribution of the largest eigenvalue in principal components analysis, *The Annals of Statistics* 29 (2) (2001) 295 – 327.
- [41] P. Stoica, Y. Selen, Model-order selection: a review of information criterion rules, *IEEE Signal Processing Magazine* 21 (4) (2004) 36–47. doi:10.1109/MSP.2004.1311138.
- [42] M. E. Tipping, C. M. Bishop, Probabilistic principal component analysis, *Journal of the Royal Statistical Society. Series B (Statistical Methodology)* 61 (3) (1999) 611–622.
- [43] A. Aubry, A. De Maio, S. Marano, M. Rosamilia, Structured covariance matrix estimation with missing-data for Radar applications via Expectation-Maximization, *arXiv preprint arXiv:2105.03738* (2021).
- [44] D. Paindaveine, A canonical definition of shape, *Statistics & probability letters* 78 (14) (2008) 2240–2247.
- [45] T. Anderson, *An Introduction to Multivariate Statistical Analysis*, Wiley, New York, 1965.
- [46] B. Kang, V. Monga, M. Rangaswamy, Rank-constrained maximum likelihood estimation of struc-

- tured covariance matrices, *IEEE Transactions on Aerospace and Electronic Systems* 50 (1) (2014) 501–515. doi:10.1109/TAES.2013.120389.
- [47] Y. Sun, P. Babu, D. P. Palomar, Robust estimation of structured covariance matrix for heavy-tailed elliptical distributions, *IEEE Transactions on Signal Processing* 64 (14) (2016) 3576–3590. doi:10.1109/TSP.2016.2546222.
- [48] M. Razaviyayn, M. Hong, Z.-Q. Luo, A unified convergence analysis of block successive minimization methods for nonsmooth optimization, *SIAM Journal on Optimization* 23 (2) (2013) 1126–1153.
- [49] P. Royston, Multiple imputation of missing values, *The Stata Journal* 4 (3) (2004) 227–241.
- [50] R. Bhatia, Positive definite matrices, Princeton university press, 2009.
- [51] F. Bouchard, A. Mian, J. Zhou, S. Said, G. Ginolhac, Y. Berthoumieu, Riemannian geometry for compound Gaussian distributions: Application to recursive change detection, *Signal Processing* 176 (2020) 107716. doi:https://doi.org/10.1016/j.sigpro.2020.107716.
- [52] J. P. Musial, M. M. Verstraete, N. Gobron, Technical note: Comparing the effectiveness of recent algorithms to fill and smooth incomplete and noisy time series, *Atmospheric Chemistry and Physics* 11 (15) (2011) 7905–7923. doi:10.5194/acp-11-7905-2011.
- [53] A. M. Zoubir, V. Koivunen, Y. Chakhchoukh, M. Muma, Robust estimation in signal processing: A tutorial-style treatment of fundamental concepts, *IEEE Signal Processing Magazine* 29 (4) (2012) 61–80.
- [54] A. Hippert-Ferrer, Y. Yan, P. Bolon, EM-EOF: Gap-filling in incomplete SAR displacement time series, *IEEE Trans. Geosci. Remote Sens.* 59 (7) (2021) 5794–5811.
- [55] G. Lerman, M. McCoy, J. A. Tropp, T. Zhang, Robust computation of linear models, or how to find a needle in a haystack, Tech. rep., California Inst of Tech Pasadena Dept of Computing and Mathematical Sciences (2012).
- [56] J. Chen, X. Zhu, J. E. Vogelmann, F. Gao, S. Jin, A simple and effective method for filling gaps in Landsat ETM+ SLC-off images, *Remote sensing of environment* 115 (4) (2011) 1053–1064.
- [57] P. Rakwatin, W. Takeuchi, Y. Yasuoka, Restoration of Aqua MODIS band 6 using histogram matching and local least squares fitting, *IEEE Transactions on Geoscience and Remote Sensing* 47 (2) (2008) 613–627.
- [58] M. Rußwurm, C. Pelletier, M. Zollner, S. Lefèvre, M. Körner, Breizhcrops: A time series dataset for crop type mapping, *International Archives of the Photogrammetry, Remote Sensing and Spatial Information Sciences ISPRS* (2020) (2020).
- [59] A. Barachant, S. Bonnet, M. Congedo, C. Jutten, Multiclass brain–computer interface classification by riemannian geometry, *IEEE Transactions on Biomedical Engineering* 59 (4) (2012) 920–928. doi:10.1109/TBME.2011.2172210.
- [60] M. Congedo, P. L. C. Rodrigues, C. Jutten, The riemannian minimum distance to means field classifier, in: 8th Graz Brain-Computer Interface Conference 2019, 2019.
- [61] S. Vassilvitskii, D. Arthur, k-means++: The advantages of careful seeding, in: Proceedings of the eighteenth annual ACM-SIAM symposium on Discrete algorithms, 2006, pp. 1027–1035.
- [62] M. F. Baumgardner, L. L. Biehl, D. A. Landgrebe, 220 band aviris hyperspectral image data set:

June 12, 1992 indian pine test site 3, Purdue University Research Repository 10 (2015).